Afterglow and thermoluminescence properties of Lu_2SiO_5:Ce scintillation crystals

1994 J. Phys.: Condens. Matter 6 4167

(http://iopscience.iop.org/0953-8984/6/22/016)

J. Phys.: Condens. Matter 6 (1994) 4167–4180. Printed in the UK

Afterglow and thermoluminescence properties of Lu_2SiO_5:Ce scintillation crystals

P Dorenbos†, C W E van Eijk†, A J J Bos‡ and C L Melcher§

† Delft University of Technology, Faculty of Applied Physics, IRI, Mekelweg 15, 2629 JB Delft, The Netherlands.

‡ Interfaculty Reactor Institute, Delft University of Technology, c.o IRI, Mekelweg 15, 2629. JB Delft, The Netherlands

§ Schlumberger–Doll Research, Old Quarry Road, Ridgefield, CT 06877-4108, USA

Received 21 December 1993

Abstract. The afterglow and thermoluminescence (TL) properties of several Ce^{3+} doped Lu_2SiO_5 crystals are reported. Both properties are caused by the presence of charge traps in the crystals. At least six different glow peaks are observed in the TL glow curve. Each is related to a specific charge trap. The parameters for these charge traps, such as the trap depth and the frequency factor, were obtained from first-order kinetics peak analysis of the TL glow curve. A charge trap with a depth of 1.0 eV is responsible for the afterglow observed at room temperature. Ce^{3+} ions appear to be the luminescence centres in the recombination process of the trapped charge carriers. It will be shown that optical excitation in the 5d levels of Ce^{3+} produces trap filling. The possible nature of the charge traps will be discussed.

1. Introduction

One of the first studies on Ce^{3+} doped Lu_2SiO_5 material was reported in 1969 by Gomes de Mesquita and Bril [1]. These authors studied the luminescence of Lu_2SiO_5:Ce^{3+} (LSO:Ce) powder for its potential application as a cathode ray tube phosphor. Its luminescence near 410 nm is caused by the dipole allowed transition from the lowest 5d excited level to the two levels of the $4f^1$ ground state configuration of Ce^{3+} ions. Not until the work by Melcher and Schweitzer [2, 3, 4] was the potential application as a scintillation crystal realized. A unique combination of a high density (7.4 g cm^{-3}), a fast scintillation decay time (~40 ns), and a large scintillation light yield (60–70% relative to NaI(Tl^+)) makes Lu_2SiO_5:Ce^{3+} crystals suitable for the fast detection of high-energy gamma rays. Besides studies of the applicability of Lu_2SiO_5:Ce^{3+} crystals in radiation detectors [4], studies of the scintillation/luminescence mechanism have been reported [5, 6].

Although LSO crystals show good scintillation properties, they also show a fairly strong afterglow. In some applications this may be an annoying property. In order to investigate the afterglow mechanism, scintillation and thermoluminescence properties were studied. A second reason to perform these experiments was the observation that while most LSO:Ce crystals grown to date have good scintillation properties, a few crystals show a very low scintillation light output for unknown reasons. It was hoped that the study of TL could reveal the origin of the poor scintillation properties in these crystals. In summary, we were interested in the relation between afterglow, TL glow peaks and scintillation properties. In this work, we concentrate on the first two properties. The scintillation properties of the crystals will be presented elsewhere [7, 8].

0953-8984/94/224167+14$19.50

2. Experimental techniques

The crystals studied in this work were grown by Schlumberger–Doll Research in nitrogen atmosphere containing 3000 ppm oxygen employing the Czochralski technique. We refer to Melcher *et al* [2, 3, 4, 9] for additional information on the properties of the raw materials used, the method of crystal growth and the physical properties of LSO:Ce crystals. We have studied three different samples each from a different crystal boule. The growth rate and the nominal Ce^{3+} concentration in the melt (in at.% relative to Lu^{3+}) are shown in table 1. Figure 1 shows the optical absorption spectrum typical of LSO:Ce crystals. The absorption bands at 356, 295, 264 and 220 nm are caused by 4f–5d transitions in the Ce^{3+} ions. The actual Ce concentration was estimated from the absorption coefficient, μ, of the band at 356 nm. This concentration is considerably lower than the concentration in the melt because of a low crystal to melt distribution coefficient [9]. Table 1 also shows some scintillation properties such as the light yield and decay time. The LSO7-11 and LSO6-4 crystals are characteristic of the best, in terms of scintillation properties, LSO:Ce crystals grown so far. The LSO32b sample was studied because it shows very poor scintillation properties.

Table 1. Properties of three LSO:Ce scintillation crystals. The Ce^{3+} concentrations are in at.% relative to the Lu^{3+} concentration. μ is the optical absorption coefficient at 356 nm. The light yields in photons MeV^{-1} pertain to excitation with 662 keV γ-rays [7, 8]. τ is the $1/e$ decay time of γ-ray excited scintillation pulses. The value for LSO32b is an approximation to a non-exponentially decaying scintillation pulse.

	LSO32b	LSO7-11	LSO6-4
Growth rate (mm hr^{-1})	2	0.5	0.5
Ce concentration in melt (at.%)	0.13	0.25	0.12
μ (cm^{-1})	27	36	14
Ce^{3+} concentration (at.%)	0.036	0.048	0.019
Photons MeV^{-1}(662 keV)	660	22 000	25 000
τ (ns)	35 (non-exponential)	41±2	37±2

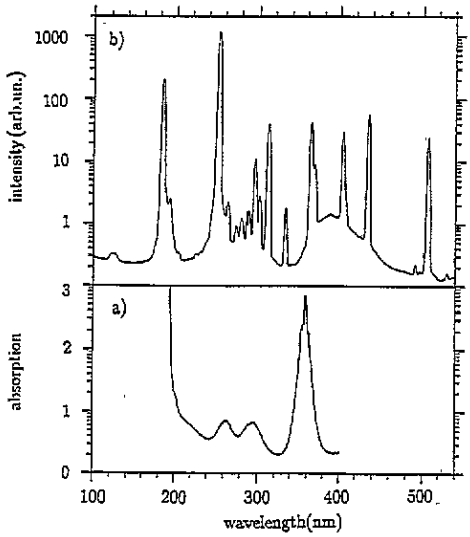

Figure 1. (a) Optical absorption ($-{}^{10}\log$(transmission)) spectrum of a 1.90 mm thick LSO32b crystal. (b) Hg lamp emission spectrum. The 185 and 254 nm lines reappear in the spectrum at 370 and 508 nm due to second-order transmission by the monochromator.

Disc shaped samples with diameters of about 4 mm and thicknesses of 0.4–0.5 mm cut from the original single crystals were used in the afterglow studies and thermoluminescence (TL) experiments. The crystals were exposed either to UV light from an Oriel (model 6035) low pressure pencil type Hg lamp with a 3.8×0.5 cm aperture shield or x-rays from an x-ray tube (Philips model PW2113/00). The Hg lamp operated at a root mean square (RMS) current of about 23 mA and an RMS voltage of 70 V. It was located 30 cm from the sample under illumination. Prior to each exposure we allowed a 2 min warm up period of the Hg lamp. Its emission spectrum is shown in figure 1(a). The x-ray tube has a copper anode and was operated at 35 kV anode voltage and 25 mA anode current. During irradiation the crystals were located 127 mm from the focal spot on the copper anode. Under these conditions, a total x-ray energy of $\sim 1\times10^8$ MeV is incident on a crystal per second. The x-rays will be absorbed in a thin top layer of the crystal.

Glow curves (TL as a function of temperature) were measured in an N_2 atmosphere at heating rates varying from 0.24 to 6 K s^{-1} using a modified microprocessor controlled Harshaw 2000 TL reader which has been described elsewhere [10]. This reader is equipped with an EMI9757B photomultiplier tube (PMT). Heater element temperature and PM signal were recorded every 0.125 s. The glow curves were analysed with a curve fitting program for thermally activated processes [11]. This program uses a linear least-squares minimization procedure to determine the peak area, activation energy and frequency factor of all peaks in the glow curve.

TL emission spectra were measured using a high-sensitivity TL spectrometer developed at Delft [12]. In this reader, the TL emission spectrum is continuously measured in the 250–750 nm range using a dispersive grating and an intensified diode array (512 elements) as detector. Emission spectra were stored every 0.71 s (e.g. at 3.6 K intervals if a heating rate of 5 K s^{-1} is employed). A 1 mm entrance slit was used resulting in a wavelength resolution of 29 nm.

The following equation describes the first-order kinetics glow peak $I(T)$

$$I(T) = n_0 s \exp\left(-\frac{E}{k_B T}\right) \exp\left(-\frac{s}{\beta}\int_{T_0}^{T} \exp\left(\frac{-E}{k_B T'}\right) dT'\right) \tag{1}$$

with n_0 the number charge carriers involved in the thermoluminescence, s the frequency factor which is of the order of lattice vibrational frequencies, E the trap depth also called activation energy, k_B the Boltzmann constant, β the constant heating rate and T_0 the starting temperature of the TL glow curve [13].

3. Results

3.1. After glow

Two, in principle quite similar, methods were employed to study the afterglow properties of the $Lu_2SiO_5:Ce^{3+}$ crystals. In one method, a crystal is annealed for several minutes at 672 K. After cooling to room temperature, the crystal is exposed to Hg lamp light. The crystal was, within 1–3 min after exposure, optically coupled to the window of a Philips XP2020Q PMT and covered with a white reflecting Teflon tape in order to obtain optimal light collection on the photocathode. Since the gain and the quantum efficiency of the employed XP2020Q photomultiplier tube were known, an estimate for the absolute afterglow intensity at room temperature in photons s^{-1} was obtained. Note that the above method is quite similar to the one used to determine the absolute light yield of scintillation crystals [14].

Figure 2 shows the afterglow, normalized per mg of crystal material, of the three crystals as a function of time. LSO7-11 and LSO6-4 show an exponentially decaying afterglow with

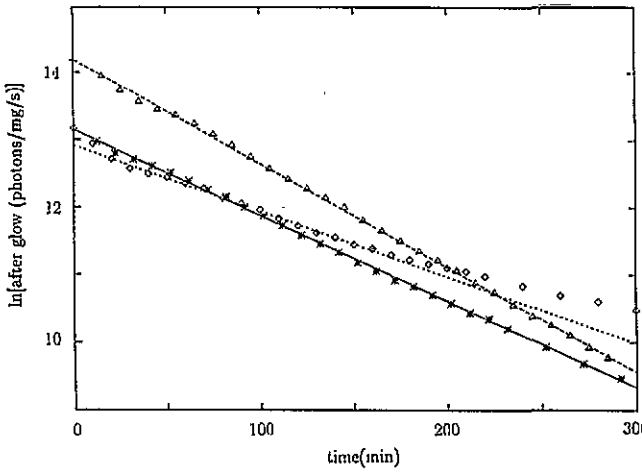

Figure 2. After glow luminescence of the (*) LSO7-11 (57 mg), (Δ) LSO6-4 (35 mg), and (◇) LSO32b (30 mg) crystals at temperatures of 298, 300 and 300 K, respectively. The crystals were exposed for 4, 15 and 4 s to the Hg lamp light, respectively. The straight lines through the data are least-squares fits. In the case of the LSO32b crystal only the data between 20 and 180 min were used in the least-squares fit.

1/*e* decay times of 4730 and 3900, respectively. The afterglow of LSO32b is roughly described by a decay time of 6150 s during the first 3 h after illumination. Beyond 3 h the afterglow decays non-exponentially.

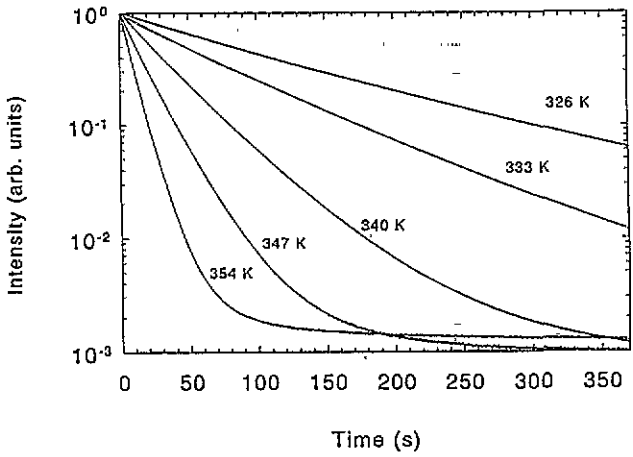

Figure 3. Normalized isothermal afterglow decay curves for the LSO7-11 crystal at five temperatures.

In the second method, a crystal is also heated to 672 K and after cooling to room temperature exposed to Hg lamp light. The afterglow is recorded at elevated but constant temperature employing the TL set-up. Figure 3 shows the so called isothermal afterglow decay curves for the LSO7-11 crystal. One observes a more or less exponentially decaying afterglow intensity with a decay time which decreases with increasing temperature. Such behaviour indicates a thermally activated mechanism for the afterglow with a decay time expressed by

$$\tau = \tau_0 \exp\left(\frac{E}{k_B T}\right) \tag{2}$$

τ_0 is a constant with a value of the order of the period of lattice vibrations and E is the activation energy. Figure 4 shows an Arrhenius plot in which results of both methods are summarized. A least-squares fit of (2) to the data yields $E = 1.01 \pm 0.03$ eV and $\ln[\tau_0^{-1}(\mathrm{Hz})] = 30.8 \pm 0.9$.

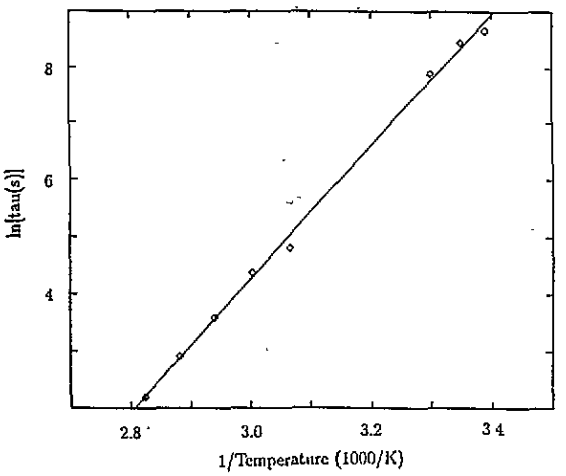

Figure 4. Arrhenius plot of the isothermal afterglow decay time. Solid line, least-squares fit to the data yielding parameters E = 1.0 eV and $\tau_0^{-1}=2.5\times10^{13}$ Hz.

The afterglow at 354 K, see figure 3, shows two afterglow decay components. The fast component is dominant in the first 50 s and the slow component dominates beyond 100 s. We will show later that this slow component is related to a thermally activated process with a larger activation energy.

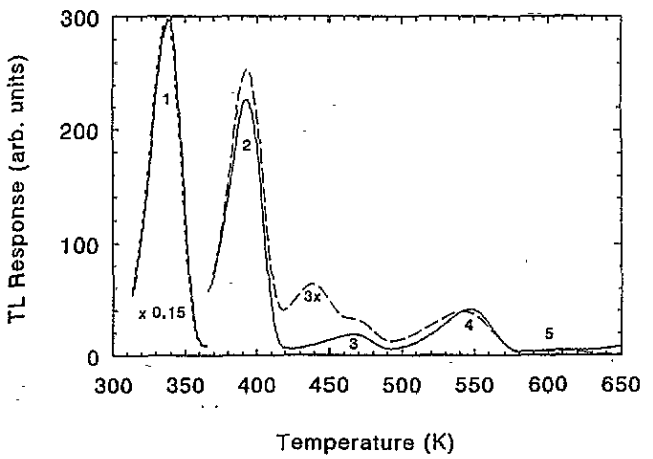

Figure 5. TL glow curves of the LSO7-11 crystal recorded at a heating rate β=0.24 K s^{-1}. The solid curve is obtained after exposure for 40 s to Hg lamp light and the dashed curve after exposure for 30 s to x-rays. For illustration purposes both curves are normalized to the height of peak 1. Moreover, peak 1 is multiplied by a factor of 0.15.

3.2. Thermoluminescence

Figure 5 shows thermoluminescence glow curves for the LSO7-11 crystal. After exposure to Hg lamp light, five glow peaks are observed. In order of appearance, the peaks are numbered from 1 to 5. The first four are clearly visible. The fifth, near 610 K, becomes more visible if the exposure time is increased. Upon exposure of the crystal to x-rays, in addition to these five glow peaks, a sixth peak, hereafter referred to as peak 3x, is observed.

Figure 6 shows the thermoluminescence of the LSO7-11 crystal as a function of both the temperature and the wavelength. The crystal was first heated to a temperature of 723 K. After cooling to room temperature, the crystal was irradiated for 70 s with x-rays and then heated to 363 K. During this heating phase the traps responsible for peak 1 in figure 5 are emptied. Subsequently, starting at 300 K, the spectrum of figure 6 was recorded. Peaks 2, 3x, 3, 4 and 5, and although not visible in figure 6 also peak 1, each show an

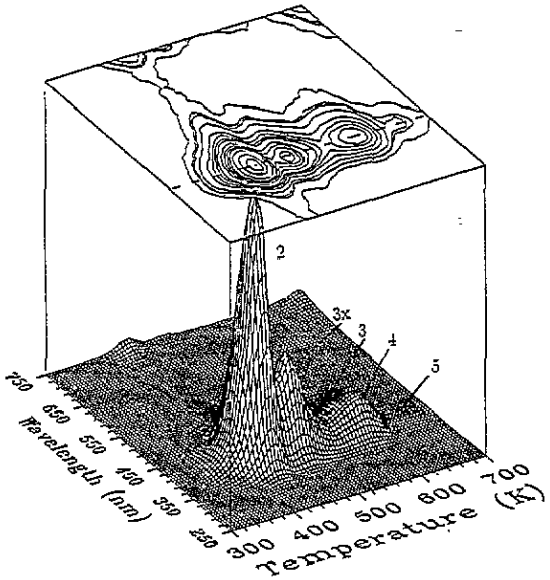

Figure 6. Thermoluminescence of the LSO7-11 crystal as a function of both the temperature and the wavelength after 70 s exposure to x-rays. Peak 1 is absent due to a peak cleaning technique. A heating rate of 5 K s^{-1} was employed. Second-order transmission of the monochromator is responsible for the luminescence near 750 nm. The wavelength resolution is 29 nm. The contour plot illustrates that each TL peak has the same emission band near 420 nm.

emission spectrum characteristic of Ce^{3+} 5d–4f luminescence near about 420 nm. From these emission spectra, we conclude that the Ce^{3+} ions are the recombination centres for the de-trapped charge carriers.

Before analysing the TL glow curves, the curves must be corrected for thermal quenching of the Ce^{3+} luminescence. The quenching, $Q(T)$, is described by:

$$Q(T) = \frac{\Gamma_\nu}{\Gamma_\nu + \Gamma_q(T)} \qquad (3)$$

with $\Gamma_\nu = 2.3\times10^7$ Hz the radiative decay rate of Ce^{3+}, $\Gamma_q = \Gamma_0 \exp(-E/k_BT)$ is the thermally activated quenching rate with $\ln[\Gamma_0(\mathrm{Hz})]=27.4\pm1.7$ and $E = 0.32\pm0.02$ eV. The values for Γ_0/Γ_ν and E were obtained by studying the Ce^{3+} luminescence intensity as a function of the temperature. Knowing these values and since $\tau(\mathrm{RT})=(\Gamma_\nu+\Gamma_q(\mathrm{RT}))^{-1}$, Γ_0 and Γ_ν were calculated separately from the known Ce^{3+} scintillation decay time of $\tau(\mathrm{RT})=40$ ns at room temperature (RT). With these parameters, e.g. Q-values of 0.23 and 0.014 are obtained at 400 and 600 K, respectively.

3.3. Glow peak analysis

In order to obtain reliable parameters for the traps responsible for the TL glow peaks, we measured TL glow curves at different heating rates and different exposure times either to Hg lamp light or to x-rays. Figure 7 shows TL glow curves of the LSO7-11 crystal; the exposure time to x-rays varies from 5 s to 180 s. The positions of peak 1, peak 2, peak 3x, probably peak 3, and peak 5 are independent of the exposure time. Peak 4 appears to shift towards lower temperatures as its intensity increases, see the inset in figure 7. This behaviour is not described by first-order kinetics, see (1), which predicts a peak position independent of its intensity [15]. Similar experiments with Hg lamp light illumination showed more clearly *that the position of peak 3 is independent of its intensity.*

Figure 8 shows the same glow curve as the one shown in figure 5, but now the curve has been corrected for thermal quenching. The six solid curves are results obtained by fitting the TL glow curve with six first-order kinetics glow peaks.

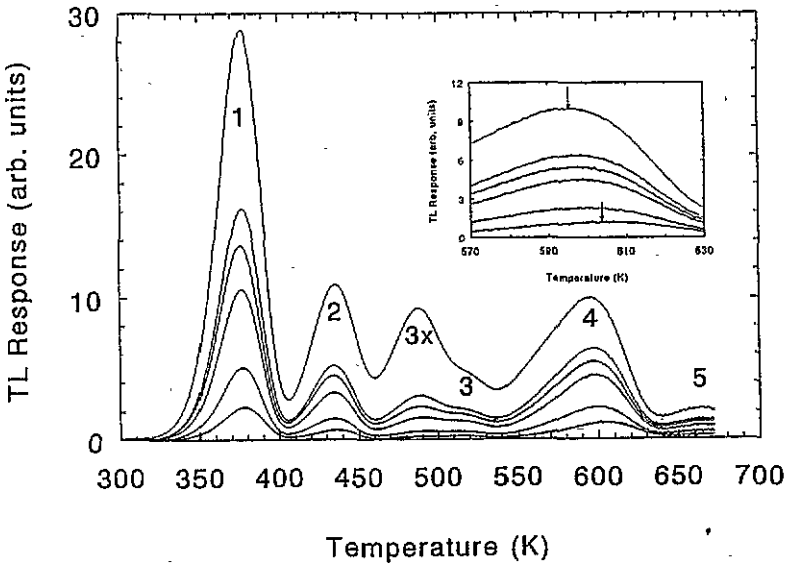

Figure 7. Thermoluminescence glow curves of LSO7-11 for, in order of increasing intensity, x-ray exposure times of 5, 10, 20, 30, 40 and 180 s. The curves were recorded at a heating rate of 6 K s^{-1} and are corrected for thermal quenching of the luminescence.

Table 2 compiles results for the LSO7-11 crystal obtained from glow curve analysis of many TL glow curves. In each case the TL peaks were fitted with the equation for the first-order kinetics glow peak. Consistent parameters were obtained for peak 1 and peak 2. Variation of the heating rate by a factor of 25 from 0.24 K s^{-1} to 6 K s^{-1} yields almost the same parameters for peak 1 and peak 2. The parameters are also independent of the exposure time to either x-rays or Hg lamp light resulting in peak intensity changes of several orders of magnitude. Concluding, peak 1 and peak 2 are well described by first-order kinetics glow curves. The third and fourth rows compile results from analysis of peaks 3x and 3 in TL glow curves after x-ray exposure of the crystal. It is difficult to distinguish peak 3 from peak 3x, see also figure 7, which results in rather inaccurate parameter values for these two peaks. The results for peak 3 in TL glow curves after Hg lamp light exposure of the sample are considered to be more reliable. The parameter values for peak 4 depend on the intensity of the peak. The smallest E and s values in table 2 are obtained for the TL curve of a 180 s x-ray exposed crystal; the largest values are obtained for the shortest exposed (5 s) one; both TL curves can be seen in figure 7. Clearly, peak 4 is not correctly described by first-order kinetics. Parameters for peak 5 were only obtained for heating rates of 0.24 and 1 K s^{-1}. If a heating rate of 6 K s^{-1} is used, peak 5 falls beyond the temperature range of our equipment. In addition to the error sources described above there may be a systematic error due to the error in the correction for thermal quenching of the Ce^{3+} luminescence. An error in the activation energy for thermal quenching is reflected directly in the obtained value for the trap depth and frequency factor.

3.4. TL glow peak intensities

TL glow curves for the LSO7-11 and LSO6-4 crystals were recorded at β=6 K s^{-1} as a function of the exposure time to Hg lamp light. Figure 9 shows the integral intensities of peaks 1, 2, 3 and 4 for the LSO7-11 crystal. The glow curves were not corrected for thermal quenching of Ce luminescence. The origin of the absolute scale along the vertical

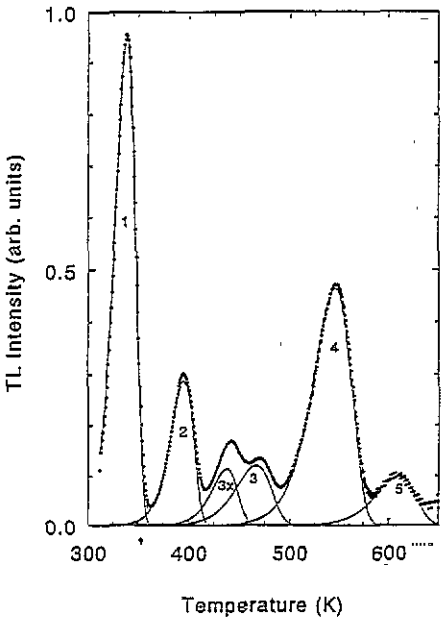

Figure 8. Thermoluminescence glow curve of LSO7-11 after 30 s exposure to x-rays. The heating rate was 0.24 K s^{-1} and the curve has been corrected for thermal quenching of Ce^{3+} luminescence. The six solid curves are results obtained with first-order kinetics glow peak fitting of the six glow peaks.

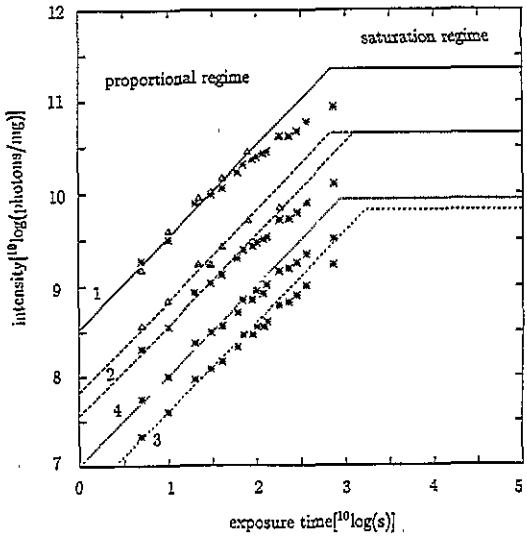

Figure 9. TL peak intensities of the LSO7-11 crystal as a function of the exposure time to Hg lamp light. A heating rate of 6 K s^{-1} was employed and the results are not corrected for the quenching of Ce^{3+} luminescence. *, results after an anneal at 672 K with all traps empty, and the TL glow curves recorded up to a temperature of 672 K. Δ, results obtained with traps 3, 4, and deeper traps filled to saturation, and the TL glow curves recorded up to a temperature of 492 K. The lines with unit slope are least-squares fits to the data points below 100 s. The horizontal lines in the saturation regime represent the saturation level determined from high-intensity Hg lamp light exposed crystals.

Table 2. 2: Results from first-order kinetics glow curve fits on TL glow curves for the LSO7-11 crystal. The stochastic errors are about ΔE = 0.02 eV and $\Delta \ln[s(\mathrm{Hz})]$=0.5. In addition there is a systematic error of about the same size due to the error in the correction for thermal quenching of the luminescence.

	β=0.24 K s^{-1}		β=1.0 K s^{-1}		β=6.0 K s^{-1}	
Peak	E (eV)	$\ln[s(\mathrm{Hz})]$	E (eV)	$\ln[s(\mathrm{Hz})]$	E (eV)	$\ln[s(\mathrm{Hz})]$
1	0.957	29.0	0.980	29.6	0.981	29.3
2	1.174	30.6	1.171	30.5	1.173	30.5
3x[a]	1.254	29.3	1.397	33.1	1.410	33.1
3[a]	1.051	21.8	0.904	18.8	0.907	19.5
3[b]	1.200	25.6	1.258	27.1	1.299	28.4
4	E=1.1–1.5 eV and $\ln[s(\mathrm{Hz})]$=20.2–26.7					
5	1.604	26.1	1.758	29.4	—	—

[a] In TL glow curves of x-ray exposed crystals.
[b] In TL glow curves of Hg lamp light exposed crystals.

axes will be discussed later. Up to 100 s exposure time, the intensity of the peaks grows

proportionally with the exposure time and there is a constant intensity ratio of 100:11:1.3:3 between the peaks 1, 2, 3 and 4, respectively. Beyond about 200 s the growth rate of the peaks starts to decrease and saturation effects start to appear. For long exposure times at a short distance from the Hg lamp, the intensities of the TL-peaks saturate to values independent of the exposure time and the illumination intensity. In the saturation regime, the intensity ratio of the peaks has changed to 100:20:3:3.8. So, the intensities of peaks 2 and 3 have increased significantly relative to those of peaks 1 and 4.

In a second series of experiments, the crystal was first exposed for several minutes to intense Hg lamp light causing a saturation of trap filling. Next the TL glow curve was recorded up to a temperature of 492 K with a heating rate of 6 K s^{-1}. As can be observed in figure 7, which pertains to TL glow curves also recorded at 6 K s^{-1}, only the charge traps responsible for peak 1 and peak 2 will be emptied. The deeper traps corresponding to peaks 3, 4 and 5 will remain filled. After this first TL read-out, the intensities of peak 1 and peak 2 were studied as functions of the exposure time to the Hg lamp. A heating rate of 6 K s^{-1} was used up to a temperature of 492 K. So, the traps responsible for peak 3 and peak 4 remain filled during these TL measurements. Figure 9 shows that under these conditions the absolute intensity of peak 1 behaves similarly as in the case in which the traps for peak 3 and peak 4 are empty. Peak 2, however, shows in the proportional regime almost twice the intensity. Note that the intensity ratio of peak 1 to peak 2 is 100:20 which is the same as the ratio observed in the saturation regime in the first series of experiments.

3.5. Conditions for trap filling

3.5.1. Results on the LSO7-11 crystal after an anneal at 672 K. By means of a monochromator a single emission line of the Hg lamp spectrum, see figure 1, was selected, and the sample was exposed to it. The lines at 185, 254, 313 and 365 nm each yield, apart from the intensity, TL glow curves similar to the one shown in figure 5 (solid curve). The emission lines at 404 and 436 nm do not produce any TL effects. Apparently there is a threshold located somewhere between 365 and 404 nm. Beyond this threshold, the photon energy is too small to release the charges needed for filling the traps. Since this threshold corresponds with the threshold for optical absorption due to the 4f–5d transition in Ce^{3+} ions, see figure 1, we conclude that trap filling proceeds via excitation of 4f electrons to the 5d levels of Ce^{3+}.

3.5.2. Results on the LSO7-11 crystal after first being exposed to intense Hg lamp light which causes saturation, and next heated to à temperature of 492 K. The traps responsible for peaks 1 and 2 are then empty and the deeper traps are filled. After this treatment, the crystal was illuminated for 5 min at a distance of 3.5 cm from the Hg lamp and with a glass (Schott GG495) optical filter between the crystal and the Hg lamp. Under these conditions only photons with wavelength longer than about 495 nm are incident on the crystal and 4f–5d transitions in Ce^{3+} are not possible. The TL glow curve shows, nevertheless, glow peak 1 and glow peak 2 with intensities of 4.7×10^8 photons mg^{-1} and 9.2×10^7 photons mg^{-1}, respectively. Note that the intensity ratio (100:20) is the same as the ratio observed in the saturation regime. The same experiment performed on the sample with all traps empty did not result in any filling of traps 1 and 2.

3.6. Results for the LSO6-4 and LSO32b crystal

The LSO6-4 crystal shows a TL-glow curve quite similar to the one observed for the LSO7-11 crystal. In the proportional regime, the intensity ratios of peaks 1, 2, 3 and 4, using

a heating rate of 6 K s^{-1}, were found to be 100:13.9:2.2:3.7. In the saturation regime, a ratio of 100:19:3.4:3.9 was observed. The absolute intensity of peak 1 amounted to 1.3×10^{8} photons mg^{-1}/(1 s exposure time) in the proportional regime and to 1.2×10^{11} photons mg^{-1} in the saturation regime.

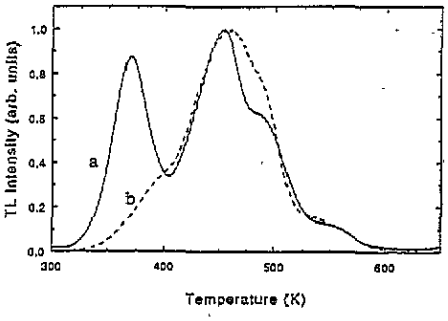

Figure 10. TL glow curve of the LSO32b crystal after 10 s (a) and 180 s (b) illumination time with a Hg lamp. A linear heating rate of 6 K s^{-1} was used and the glow curves are corrected for thermal quenching. Glow curve b is scaled down by a factor of 840 relative to glow curve a.

Figure 10 shows the TL glow curve of the LSO32b crystal after exposure to Hg lamp light. The glow curve is totally different from those of the LSO7-11 and LSO6-4 crystals. At least four peaks, each caused by Ce^{3+} luminescence can be distinguished. Furthermore, in contrast to the other two crystals, the shape of the glow curve changes and its integrated intensity grows supralinearly with the exposure time. The complexity of the TL glow curve did not allow us to obtain reliable parameters for the charge traps in the LSO32b crystal.

4. Discussion

We limit the discussion mainly to the afterglow and thermoluminescence of the crystals showing good scintillation properties (LSO7-11 and LSO6-4). These crystals exhibit, for β=0.24 K s^{-1} and after exposure to UV light, five glow peaks between room temperature and 650 K. There is also an indication of a sixth glow peak at still higher temperatures [16]. It is quite clear that the afterglow exhibited by these crystals is related to peak 1. The parameter values obtained from fitting (1) to this glow peak, see table 2, are within accuracy equal to the parameters obtained from the Arrhenius plot of the isothermal decay time, see figure 4. Since two independent techniques provide the same parameter values, this also demonstrates that peak 1 is well described by first-order kinetics. The presence of a slow afterglow decay component observed in figure 3 for the afterglow recorded at 354 K must be related to peak 2 in the TL glow curve.

The LSO32b crystal shows an afterglow decay curve which is different from those observed for the other LSO crystals, see figure 2. This is related to the deviating TL glow curve shown in figure 10.

The time integral of the isothermal afterglow, e.g. as shown in figure 2 for the 4 s Hg lamp light exposed LSO7-11 crystal, should if the thermal quenching of Ce luminescence is properly accounted for, be equal to the temperature integral of glow peak 1 in the TL glow curve of the same sample after the same exposure time. The same holds for the LSO6-4 crystal. In fact, this has been used to obtain the absolute scale along the vertical axes of figure 9 in terms of photons emitted per milligram of LSO material. By multiplying the intensities of peaks 1, 2, 3 and 4 by factors of 2.8, 7.1, 22.9 and 67.9, respectively, a correction is made for the thermal quenching of Ce^{3+} luminescence, and values for the number of filled traps are obtained. Summing the four values yields in the saturation regime, 1.7×10^{12} for the total number of filled traps per milligram of LSO7-11 material. This implies

that 0.13% of the Ce^{3+} ions are involved in the recombination of the trapped electrons with the trapped holes. For the LSO6-4 crystal a total number of 9.3×10^{11} filled traps mg^{-1} is obtained which amounts to 0.19% of the Ce^{3+} concentration.

Formally, there are two possible origins for the charge traps: (i) extrinsic impurities incorporated in the crystal during crystal growth; (ii) intrinsic defects such as oxygen vacancies, divalent or tetravalent Ce impurities or clusters of Ce^{3+} ions creating defective regions in the host lattice. Traps may also be created during irradiation of the crystals. To know the true nature of the charge traps would require many experiments on the defect structure of the crystals. At this moment we only can speculate about several models consistent with the observed TL properties.

4.1. Charge donor and recombination centre

To fill a trap, a charge carrier has to move from a donor centre to the trap centre. It has already been concluded that trap filling can proceed via excitation of 4f electrons to the 5d levels of Ce^{3+}. After excitation, either the 5d electron or the 4f hole is transferred to the charge trap. Since the noble gas configuration of Ce^{4+} is assumed to be more stable than Ce^{2+}, we suggest that upon illumination with Hg lamp light, the 5d electron is transferred to the trapping centre and a Ce^{4+} ion is left behind. Under the assumption that the 5d level of Ce^{3+} is located in the band gap of the host crystal, the trapping centre must necessarily be located in the near vicinity of the Ce^{3+} ion. Thermal stimulation of the trapped electron reverses the process resulting in electron–hole recombination at the same Ce^{3+} ion yielding 5d–4f luminescence. The situation of a recombination centre with a trapping centre nearby is quite common for TL materials and is known as *centre to centre recombination* [15].

In principle it is also possible that once an electron is excited to the 5d level of Ce^{3+} a second photon is absorbed causing excitation of the electron to the conduction band. Trapping is then possible by traps located far from the Ce^{3+} ion and recombination proceeds *via the conduction band.* Although we cannot entirely exclude this possibility, it seems unlikely because such *two-stage reaction processes* predict a non-proportional growth of the TL peak intensities with exposure time [17, 18], and this has not been observed yet.

4.2. Nature of the charge traps

In discussing the nature of the charge traps one has to consider the following observed facts. (i) The glow peaks 1, 2, 3 and 4 appear in a fairly constant intensity ratio despite order of magnitude variations in the absolute peak intensities. (ii) After correcting for thermal quenching of Ce luminescence, the intensity ratio of the four peaks in the saturation regime is 100:50:26:94. The intensities are therefore of the same order of magnitude. (iii) The change from the proportional to the saturation regime occurs for all four peaks at about the same Hg lamp exposure times, see figure 9. These three observations suggest that the four underlying charge traps are not independently filled but are closely related to each other. We therefore propose that the four traps and also the trap responsible for glow peak 5 are located around the same trap creating defect. Adopting the model of centre to centre recombination this defect must be located near the Ce^{3+} charge donor and recombination centre. The situation has been illustrated in figure 11(a). It shows schematically the 4f and 5d levels of Ce^{3+} in the band gap of the host crystal together with the five charge traps. Each trap should be considered as a localized electronic state separated by potential energy barriers.

We already concluded that a trap can be filled via the 5d level of Ce^{3+}; this is illustrated by path 1 in figure 11(a). Furthermore, we expect that once a trap is filled, it can be emptied

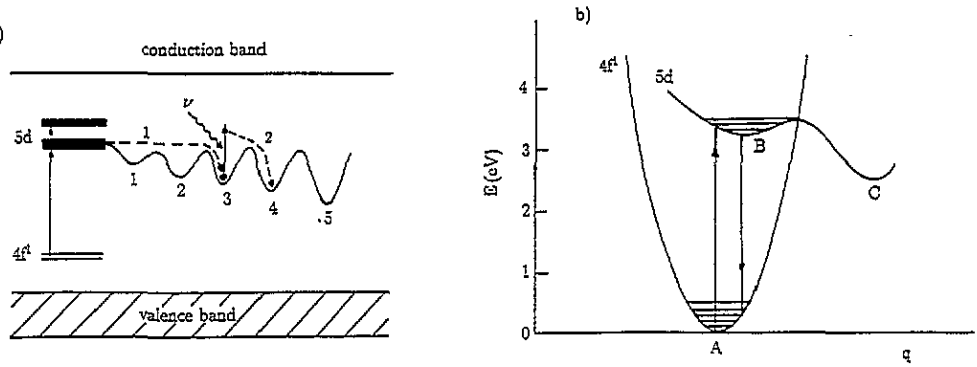

Figure 11. (a) Illustration of the proposed trapping mechanism in a centre to centre recombination model. Path 1 demonstrates trap filling, path 2 demonstrates photo stimulated de-trapping followed by trapping in another charge trap. (b) Configuration coordinate diagram illustrating possible origin of charge traps.

again by photon stimulation resulting either in re-trapping or recombination at a Ce^{3+} ion. The phenomenon of re-trapping is illustrated in figure 11(a) by path 2; an electron originally trapped at trap 3 is transferred to trap 4 by photon stimulation. The above implies that the concentration of filled traps will be determined by the equilibrium between trap filling and trap emptying. For short exposure times, trap filling dominates and the number of filled traps is expected to increase proportionally with the exposure time to Hg lamp light; this is the proportional regime in figure 9. The intensity ratios of the glow peaks are in this regime not determined by their concentration ratios, which are unity, but by the probability of electron capture by each of the five trapping levels. For long exposure times, the concentration of filled traps increases and photo-stimulated de-trapping becomes increasingly important. Eventually, in the saturation regime, equilibrium is established resulting in peak intensity ratios different from those in the linear regime. This model is also consistent with the observation that traps 1 and 2 can be filled by transfer of electrons from deeper traps under illumination by photons of wavelength longer than 495 nm.

Adopting the above described model for the TL-mechanism, we still have to discuss the nature of the trap creating defect. We envisage several possibilities: (i) an extrinsic or an intrinsic defect located in the near vicinity of the Ce^{3+} ion; (ii) the Ce^{3+} ion itself is besides the charge donor and recombination centre also the trap creating defect; (iii) a cluster of two or more Ce^{3+} ions. For the first possibility, we expect that the concentration of defects can be influenced by the crystal growth conditions, the purity of the starting materials or thermal treatments of the crystal. For the second possibility the number of traps is essentially equal to the number of Ce^{3+} ions in the lattice. For the third possibility the concentration of traps is related to the concentration of Ce clusters which may be much lower than the Ce concentration.

The ionic radius of a Ce^{3+} ion is about 10% larger than the ionic radius of the Lu^{3+} for which it substitutes [19]. Consequently, there will be a considerable relaxation of the nearest-neighbour oxygen ions surrounding the central Ce^{3+} ion. Also considering the low point symmetry (C_1) around a Ce ion [19], it is attractive to associate with each of the five charge traps a specific configuration of oxygen ions surrounding the central Ce ion. After the electron is excited to the 5d level, there is some reconfiguration of the oxygen ions resulting in a Ce^{4+} ion with the 5d electron transferred to a metastable level with mixed Ce^{3+} 5d and O^{2-} 2p character. In this model, consistent with model (ii) or (iii)

described above, the charge traps are not created until the Ce^{3+} ion has been excited to the 5d level. Considering the concentration of filled traps in the saturation regime, we observed for the LSO7-11 and the LSO6-4 crystal numbers which amount to 0.13% and 0.19% of the Ce^{3+} ion concentration. In fact these numbers are even larger if one includes the traps responsible for peak 5 and the possible presence of glow peaks at still higher temperatures. Furthermore, not 100% of the traps need to be filled in the saturation regime. Due to the equilibrium between trap filling and de-trapping by photo-stimulated luminescence it is very well possible that only a small fraction of the available traps can be filled. The observed concentration of filled traps can, therefore, be consistent with both model (ii) and model (iii).

The configuration coordinate diagram of figure 11(b) illustrates the possible nature of the charge traps. The configuration coordinate, q, represents a measure for the position (configuration) of the nearest-neighbour oxygen ions surrounding the central Ce ion. Optical excitation occurs at point A, the minimum energy of the $4f^1$ ground state. After a fast relaxation resulting in a new configuration coordinate, the system finds itself at point B from which Ce^{3+} 5d–4f emission originates. The system may also transfer to point C which represents a Ce^{4+} ion with a trapped electron nearby. It can be shown that under the condition that the electron hole recombination rate at the Ce^{3+} ion is much larger than the re-trapping rate, i.e.

$$\Gamma_v + \Gamma_q(T) \gg \Gamma_{BC.} = \Gamma_{BC,0} \exp\left(\frac{E_{BC}}{k_B T}\right) \tag{4}$$

a first-order kinetics glow curve is obtained [15]. Γ_{BC} is the transfer rate from B to C with $\Gamma_{BC,0}$ a constant of the order of the lattice vibrational frequency and E_{BC} the energy barrier between B and C. This condition is usually fulfilled for barriers larger than several tenths of an electronvolt. The fact that peak 4 is not properly described by first-order kinetics may indicate that the above condition is not met. The activation energies compiled in table 2 must, in this model, be interpreted as the barrier height between point C and B. Figure 11(b) shows one configuration coordinate. In fact there may be many different coordinates resulting a multi dimensional diagram with several local minima each corresponding to a charge trap.

The above model describes the origin of the traps responsible for glow peaks 1, 2, 3, 4 and 5 as a genuine intrinsic property of the LSO:Ce crystals. The origin of peak 3x observed upon exposure of the crystal to x-rays is probably caused by a radiation induced defect which cannot be created by low-energy photons from the Hg lamp. The LSO32b crystal shows a completely different TL spectrum from the other two crystals. Its scintillation properties are also very different. Probably this has to do with extrinsic impurities incorporated in the crystal during crystal growth. The true nature is, however, not known.

5. Conclusions

The room-temperature afterglow of LSO:Ce scintillation crystals is caused by thermally activated de-trapping of charge carriers from traps with a depth of about 1.0 eV followed by electron–hole recombination at a Ce^{3+} ion. TL studies have revealed, besides the glow curve related to the after glow, at least four other glow peaks related to deeper charge traps. The parameters for these traps were obtained employing first-order kinetics glow curve analysis. The traps can be filled by excitation of 4f electrons in Ce^{3+} to 5d levels. A *centre to centre recombination model* has been proposed to explain the observed phenomena. In this model Ce^{3+} is the charge donor, the recombination centre and also the trap creating

defect. Although no conclusive evidence has been provided, we propose that the traps are related to specific configurations of oxygen ions around the central Ce^{3+} ion. Each configuration is able to trap the 5d electron in a metastable electronic level with mixed Ce^{3+} 5d and O^{2-} 2p character; a Ce^{4+} ion is left behind. The consequence of the proposed model is that the afterglow and the presence of the charge traps are intrinsic properties of the LSO:Ce material.

Acknowledgments

There investigations in the programme of the Foundation for Fundamental Research on Matter (FOM) have been supported by the Netherlands Technology Foundation (STW). We are grateful to R A Manente for the growth of the LSO:Ce crystals.

References

[1] Gomes de Mesquita A H and Bril A 1969 *Mater. Res. Bull.* **4** 643
[2] Melcher C L and Schweitzer J S 1992 *Nucl. Instrum. Methods* A **314** 212
[3] Melcher C L and Schweitzer J S 1992 *IEEE Trans. Nucl. Sci.* NS-**39** 502
[4] Melcher C L 1992 *Conf. Record 1992 IEEE Nuclear Science Symp. Medical Imaging Conf. (Orlando, FL 1992)* p 123
[5] Suzuki H, Tombrello T A, Melcher C L and Schweitzer J S 1993 *IEEE Trans. Nucl. Sci.* NS-**40** 380
[6] Suzuki H, Tombrello T A, Melcher C L and Schweitzer J S 1992 *Nucl. Instrum. Methods* A **320** 263
[7] Dorenbos P, de Haas J T M, van Eijk C W E, Melcher C L and Schweitzer J S 1993 *Nuclear Science Symp. Medical Imaging Conf. IEEE93 (San Francisco, CA 1993)*
[8] Dorenbos P, van Eijk C W E, Bos A J J and Melcher C L 1993 *Int. Conf. on Luminescence (Storrs, CT 1993)* 1994 *J. Lumin.* at press
[9] Melcher C L, Manente R A, Peterson C A and Schweitzer J S 1993 *J. Cryst. Growth* **128** 1001
[10] Hoogenboom J E, de Vries W, Dielhof J B and Bos A J J 1988 *J. Appl. Phys.* **64** 3193
[11] Wijngaarden M H, Plaisier J and Bos A J J 1985 *Radiat. Prot. Dosim.* **11** 179
[12] Piters T M, Meulemans W H and Bos A J J 1993 *Rev. Sci. Instrum.* **69** 109
[13] Randall J T and Wilkins M H F 1945 *Proc.. R. Soc.* **184** 366
[14] Dorenbos P, de Haas J T M, Visser R, van Eijk C W E and Hollander R W 1993 *IEEE Trans. Nucl. Sci.* NS-**40** 424
[15] McKeever 1985 *Thermoluminescence of Solids* (London: Cambridge University Press)
[16] Visser R, Melcher C L and Schweitzer J 1993 private communications
[17] Inabe K and Takeuchi N 1980 *Japan. J. Appl. Phys.* **19** 1165
[18] Takeuchi N, Inabe K, Kido H and Yamashita J 1978 *J. Phys. C: Solid State Phys.* **11**
[19] Felsche J 1973 *Struct. Bonding* **13** 99